Cavity cooling of an optically trapped nanoparticle

P. F. Barker
Department of Physics and Astronomy, University College London, WC1E 6BT, United Kingdom

M. N. Shneider
Applied Physics Group, Department of Mechanical and Aerospace Engineering, Princeton University, Princeton, New Jersey 08544, USA

(Received 10 October 2009; published 23 February 2010)

We study the cooling of a dielectric nanoscale particle trapped in an optical cavity. We derive the frictional force for motion in the cavity field and show that the cooling rate is proportional to the square of oscillation amplitude and frequency. Both the radial and axial components of the center-of-mass motion of the trapped particle, which are coupled by the cavity field, are cooled. This motion is analogous to two coupled but damped pendulums. Our simulations show that the nanosphere can be cooled to e^{-1} of its initial momentum over time scales of hundredths of milliseconds.

DOI: 10.1103/PhysRevA.81.023826 PACS number(s): 37.30.+i, 37.10.Vz, 42.50.Pq

The study of micro and nanomechanical oscillators [1–4] and particularly their quantum mechanical motion [5–7] is a rapidly developing field that promises insights into the boundary between quantum and classical worlds. Also, their sensitivity to the environment appears promising for the development of chemical sensors with single-atom sensitivity [8]. Cavity optomechanics is an important area within this field in which the mechanical motion of at least one degree of freedom of an oscillator is damped or cooled by interaction with the field of an optical cavity [4,9–12]. Cooling of the mechanical motion works by coupling an optical cavity to the oscillator so that it selectively scatters blue-shifted photons of a probe beam out of the cavity with respect to the incident photons. By conservation of energy, the mechanical energy of the oscillator-cavity system is reduced. A range of optomechanical oscillators and cooling schemes have now been realized experimentally [9] and currently there is a strong impetus toward reaching the quantum regime where only a few of the quantized states of at least one degree of freedom are occupied. The cooling of atomic species using laser cooling is now well established with the creation of nanoKelvin temperature gases, which has led to the realization of quantum degeneracy in gases. For molecular and atomic species that cannot be laser cooled, cavity cooling of a trapped species appears attractive because it does not rely on the detailed internal level structure [13–15]. This scheme was already used to cool a trapped atom [16], an ion [17], and atomic gases [18].

I. INTRODUCTION

In this article we consider the cavity cooling of a nanoscale particle trapped at the center of a high-finesse Fabry-Perot cavity in a vacuum. Here a center-of-mass oscillation occurs due to trapping in the periodic potential of the interference pattern created inside the cavity, while cooling occurs by interaction with the field mediated by the cavity. Unlike many optomechanical cooling schemes that utilize radiation pressure, this scheme uses the dipole force. Cavity cooling in this way is attractive because a trapped particle can be effectively isolated from the environment. This is unlike the cooling of many cavity optomechanical schemes such as cantilever [4] or membranes [19], which are directly physically connected to a large heat bath.

We consider cavity cooling of a large polarizable particle that is trapped in the intracavity field of a high-finesse cavity by modifying the model developed for a single atom in a one-dimensional (1D) cavity [20]. Because we only consider a single trapped particle, we are able to derive a velocity-dependent frictional force for small oscillations around the antinode of the intracavity field. We then consider cooling in a realistic two-dimensional (2D) cavity that includes the damping of the axial and radial motion. We show that both degrees of freedom are coupled by the cavity field, which acts to damp them. In addition to the dipole force due to the cavity field, which acts to trap the particle, the nanoparticle is also subject to gravity, which is chosen to be along the cavity axis as shown in Fig. 1.

II. 1D COOLING OF A NANOSPHERE

To explore cavity cooling we assume a field of amplitude ξ_{ext} and frequency ω_p incident on one of the two high-finesse cavity mirrors of equal reflectivity R with conductivity σ. The linewidth of the cavity is κ and the $1/e$ lifetime of a photon in the cavity is $2\pi/\kappa$. We assume that the light is impedance matched to the cavity, that the cavity is stabilized such that only the lowest order transverse electromagnetic mode (TEM_{00}) propagates, and that the nanoparticle is trapped by the field at its beam waist at position x_n. We first determine the field within the cavity in the presence of the single dielectric particle from the 1D wave equation given by

$$\frac{\partial^2 E(x,t)}{\partial t^2} + 2\kappa\frac{\partial E(x,t)}{\partial t} - c^2\frac{\partial^2 E(x,t)}{\partial x^2} = \frac{1}{\epsilon_0}\frac{\partial^2 P(x,t)}{\partial t^2} + 2\kappa^{\text{ext}}\frac{\partial E(x,t)^{\text{ext}}}{\partial t}, \tag{1}$$

where $\kappa = \frac{\sigma}{2\epsilon_0}$ and $\kappa^{\text{ext}} = \frac{\sigma}{2\epsilon_0}{}^{\text{ext}}$.

Here $E(x,t)$ and $P(x,t)$ represent the sum of all possible allowed electric field and polarization modes for the cavity,

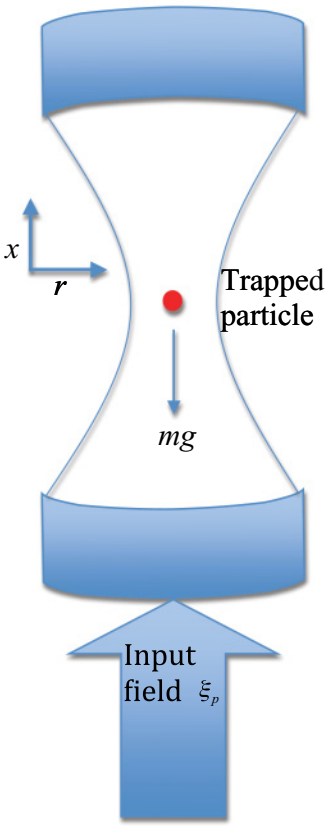

FIG. 1. (Color online) Schematic diagram for cooling a small dielectric nanoscale particle in a high-finesse cavity.

respectively. We assume that the cavity only operates on one of these modes where the electric field is $E_m(x,t) = \xi(t)(e^{-i\omega_p t} + \text{c.c.})\cos(kx)$ and the polarization is given by $P_m(x,t) = p(t)e^{-i\omega_p t} + \text{c.c.}$ in the cavity. We assume the nanoparticle is a point-like spherical particle with $P_m(x,t) = \alpha E_m(x_n,t)\delta(x-x_n)/A$ where α is the polarizability of the particle and A is the cross-sectional area of the field in the cavity. The external field that couples to this cavity mode is given by $E_m^{\text{ext}} = \xi^{\text{ext}}(t)e^{-i\omega_p t} + \text{c.c.}$ We find the equation for the evolution of field amplitude of this mode by utilizing the orthogonality of cavity modes and multiplying Eq. (1) by $E_m(x,t)$ and averaging over the cavity volume V.

Under the slowly varying envelope approximation, we obtain the 1D equation of motion for the amplitude of the single-mode field as

$$\frac{\partial \xi}{\partial t} = -\{\kappa - i[U(x_n) + \Delta]\}\xi + \kappa_{\text{ext}}\xi_{\text{ext}}, \tag{2}$$

where $U(x_n) = \frac{\alpha\omega_p \cos^2 kx_n}{\epsilon_0 V}$ is the position-dependent shift in cavity frequency induced by the polarizable particle and $\Delta = \omega_p - \omega_c$ is the cavity detuning from resonance.

The equation of motion for the momentum is simply the dipole force that results from the intracavity field acting against gravity

$$\frac{dP_{x_n}}{dt} = -\alpha|\xi|^2 k \sin 2kx_n - mg, \tag{3}$$

and the particle position is given by

$$\frac{dx_n}{dt} = P_{x_n}/m. \tag{4}$$

It is not clear from the coupled Eqs. (2), (3), and (4) that there is a dissipative force on the trapped particle in the intracavity field. To understand the damping or heating of the trapped nanoparticle we derive an equation of motion with a velocity-dependent frictional force. As we are only interested in trapped motion, we need only consider small amplitude oscillations when $kx_n \ll 1$. Additionally, because the center-of-mass motion is much smaller than the round-trip time for light in the cavity, we average Eqs. (2), (3), and (4) over a time Δt from $t - \Delta t$ to t. A suitable Δt is the cavity decay time $2\pi/\kappa$. The averaged field $\bar{\xi}$ over $2\pi/\kappa$ is given by

$$\bar{\xi} = \frac{\kappa^{\text{ext}}\xi^{\text{ext}}}{\kappa - i\left[\Delta + \frac{\alpha\omega_p}{\epsilon_0 V} + \frac{\alpha\omega_p k^2}{\epsilon_0 V}\left(v\frac{2\pi x_n}{\kappa} - x_n^2\right)\right]}, \tag{5}$$

where we now omit for convenience the subscript n for the position of the particle and the position-dependent expression for the frequency shift, now given by $U(x)$, is expanded around the nanoparticle position at $x = 0$ so that $U(x) \approx \frac{\alpha\omega_p[1-(kx)^2]}{\epsilon_0 V}$ and $x(t-\Delta t) = x(t) - 2v\pi/\kappa$, where $v = dx/dt$.

This enables us to find a time-averaged equation of motion for momentum. This is given by $\overline{\frac{dp_x}{dt}} = m\frac{d^2x}{dt^2} \approx -2\alpha k^2\bar{\xi}^2 x$, which leads to an equation of motion of the trapped nanosphere, which is a type of Liénard differential equation [21]. This is given by

$$\frac{d^2x}{dt^2} = -\Omega^2\left(x + \beta x^3 - \frac{2\pi\beta}{\kappa}x^2 v\right) - g, \tag{6}$$

where $\Omega = \sqrt{\frac{2\alpha\delta k^2}{m}}$, $\delta = \frac{|\kappa^{\text{ext}}\xi^{\text{ext}}|^2}{\kappa^2 + (\Delta + \frac{\alpha\omega_p}{\epsilon_0 V})^2}$, and $\beta = \frac{\alpha\omega_p k^2(\Delta + \frac{\alpha\omega_p}{\epsilon_0 V})}{\epsilon_0 V[\kappa^2 + (\Delta + \frac{\alpha\omega_p}{\epsilon_0 V})^2]}$. This equation differs from conventional oscillators such as the van der Pol or Duffing type in that the friction term $\frac{\beta}{\kappa}x^2$ is position dependent. When $\beta < 0$ the oscillatory motion of the sphere is damped and therefore the cavity detuning is $\Delta < -\alpha\omega_p/\epsilon_0 V$. Optimal damping or cooling of the sphere occurs when

$$\Delta_{\text{op}} = -\alpha\omega_p/\epsilon_0 V - \kappa. \tag{7}$$

Optimal heating occurs when $\Delta = -\alpha\omega_p/\epsilon_0 V + \kappa$.

An approximate expression for the energy loss rate, averaged over an oscillation period $2\pi/\Omega$, can also be determined. The rate of change in the total energy E of the particle can be determined from the power by multiplying the equation of motion (6) by mv to give $\frac{dE}{dt} = mv\frac{d^2x}{dt^2} = -m\Omega^2 xv - m\Omega^2\beta x^3 v + \frac{2\pi\beta}{\kappa}m\Omega^2 v^2 x^2 - mg$. When averaged over an oscillation period, assuming the damping is slow enough not to significantly change the amplitude of oscillations during a cycle such that $x \approx x_0 \sin(\Omega t)$, we determine a time-averaged exponential energy damping rate of

$$\Gamma = \frac{\pi\beta}{2\kappa}\Omega^2 x_0^2, \tag{8}$$

where x_0 is the amplitude of the oscillation. Note again that damping or cooling results when $\beta < 1$. Because the amplitude

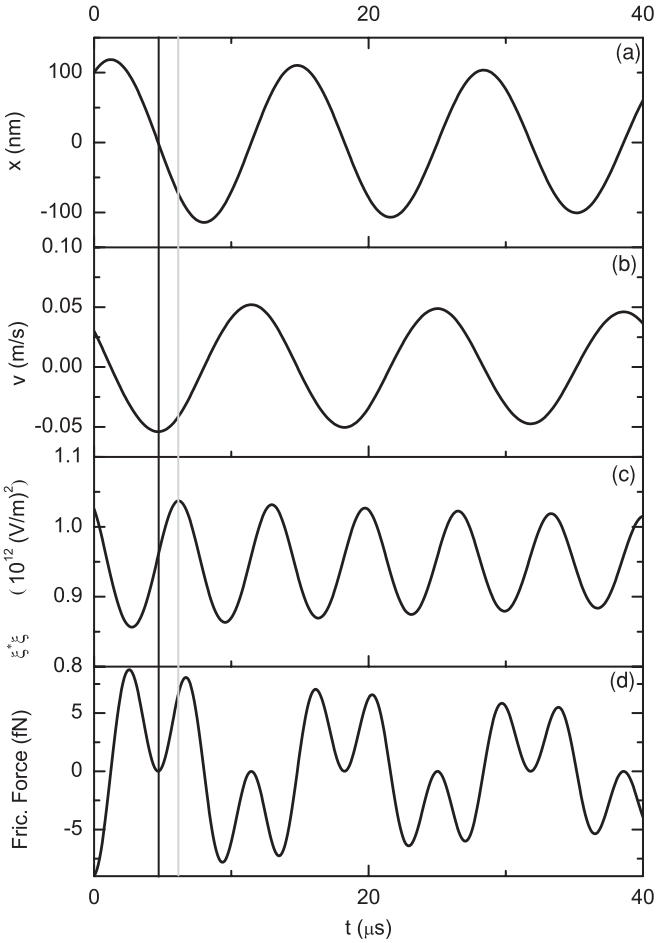

FIG. 2. A plot of the particle (a) position, (b) velocity, (c) square of field amplitude [Eq. (5)], and (d) the friction force $\frac{2\pi m\beta}{\kappa}\Omega^2 x^2 v$ derived from Eq. (6). These values are derived from the numerical solution of Eq. (6) for optimal detuning and initial particle position of 100 nm and velocity of 3 cm/s over a time of scale 40 μs.

will decrease as the particle cools at a fixed input intensity, so the damping rate also decreases, as was previously noted [22]. However, the cooling rate is proportional to the square of the oscillation frequency.

To study the cooling of nanoscale polarizable particles, we consider a SiO_2 nanosphere of radius $r = 100$ nm and refractive index of $n = 1.45$ trapped in an antinode of the intracavity field. A sphere of this size within the Rayleigh regime when $r \ll \lambda$ and can be treated as a dipole scatterer with polarizability $\alpha = 4\pi\epsilon_0 \frac{n^2-1}{n^2+2} r^3$ was determined to be 2.98×10^{-32} Cm^2 V^{-1}. Its mass, determined from its density ($\rho = 2198$ Kg m^{-3}), is $m = 9.2 \times 10^{-18}$ kg. We consider a cavity of length $L = 10$ cm with mirrors of reflectivity $R = 0.99995$ resulting in $\kappa = 4.71 \times 10^5$ rad/s. The intracavity field has a wavelength of 1064 nm with an input intensity of 1 mW and a beam radius of 50 microns in the cavity. The axial oscillation frequency for these parameters is 4.65×10^5 rad/s. The optimal detuning of the cavity from resonance is calculated from the previous parameters to be -5.0×10^5 rad/s for cooling and 4.4×10^5 rad/s for heating.

Figure 2 is a plot of the particle position and velocity as well as the square of field amplitude [Eq. (5)] and the friction force $m\frac{2\pi\beta}{\kappa}\Omega^2 x^2 v$ derived from Eq. (6). These values are derived from the numerical solution of Eq. (6) for the optimal detuning and initial particle position of 100 nm and velocity of 3 cm/s over a short time of scale 40 μs. From these plots the cooling process can be clearly understood as the trapped particle oscillates in the standing-wave field of the cavity. When the particle moves into the high intensity region (antinode) of the cavity field toward $x = 0$ there is a slight increase of the optical path length in the cavity and an increase in the position-dependent frequency shift $U(x)$. For an input field that is red-detuned from the cavity resonance, this effect pushes the cavity closer to resonance and acts to increase the intracavity intensity and thus also the dipole force on the particle. For a cavity there is a delay in the time the intracavity intensity reaches it maximum due to the motion of the particle. This difference is shown by the two vertical lines of Fig. 2. The first line marks the time when the particle reaches an antinode at $x = 0$ [Fig. 2(a)] and the second gray line when the square of the field reaches a maximum [Fig. 2(c)]. This delay has the effect of increasing the frictional force after the particle has moved past the antinode and acts to slow the particle. The same process also occurs as the particle moves in the opposite direction. Note that the frictional force is always zero at the antinode. Although not shown here, for positive detuning the effect of the position-dependent frequency shift is to tune the cavity further away from resonance. Here the lag in time for the intensity to decrease leads to heating on each half of the oscillation. It is interesting to note that for the parameters that we consider some weak cooling occurs for zero cavity detuning.

It is instructive to plot the energy damping or heating rate as a function of both detuning and position, as shown in Fig. 3. Peak negative values correspond to maximal cooling and peak positive values for maximal heating. Figure 3 also shows that the damping or heating is larger when the particle is further from the antinode of the interference pattern of the intracavity field, which has important consequences for cooling because it implies that the best damping will occur when the particle is not strongly confined and will undergo larger oscillations.

To illustrate the damped oscillatory motion of the trapped nanosphere, we plot its velocity and position for an initial

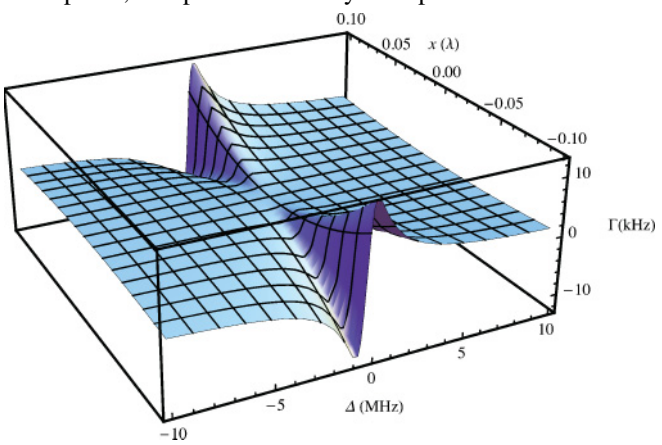

FIG. 3. (Color online) A three-dimensional plot showing the variation of the energy damping rate as a function of cavity detuning Δ and oscillation amplitude of nanosphere position x_0. Maximal cooling occurs at negative detuning.

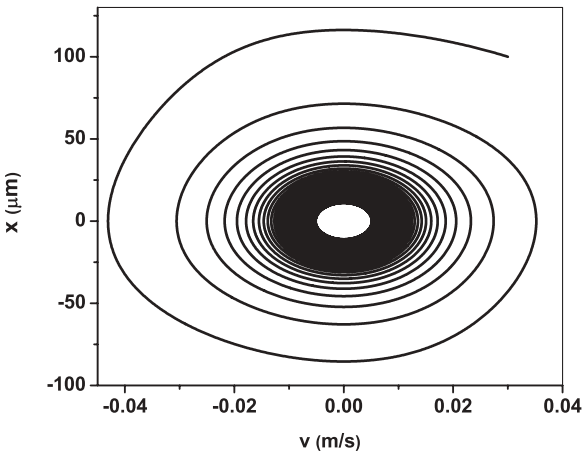

FIG. 4. A phase-space plot showing damped motion in position over 1 ms. Note that the cooling rate decreases as the particle becomes localized in the lattice potential.

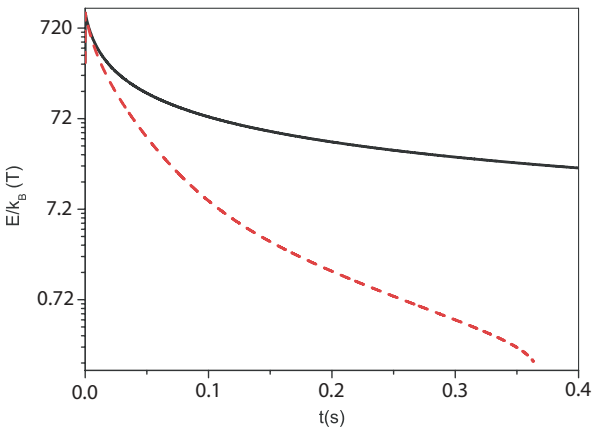

FIG. 5. (Color online) Plot of the amplitude of the oscillatory energy as a function of time to compare of cooling times for a constant input intensity into the cavity of 1 mW (solid line) and an exponentially decreasing input intensity with a e^{-1} decay constant of 50 ms (dashed).

velocity of $v = 3$ cm s^{-1}, corresponding to an initial kinetic energy of $E/k_b = 300$ K and $x = 100$ nm from the trap center with optimal cavity detuning for damping. The equations of motion were integrated in time using a fourth-order Runge-Kutta method. The damped oscillatory motion is clearly shown, even for this short time period $t = 1$ ms and there is good agreement between the simplified time-averaged equation of motion (6) and the exact model of Eqs. (2), (3), and (4). The oscillation frequency, largely determined by the input intensity, was chosen to be smaller than the cavity linewidth. However, an increase in intensity and thus oscillation frequency can be used to cool the particle in the resolved-sideband limit, which is of importance for cooling to the quantum ground state [23]. Figure 4 shows a phase-space plot of the velocity and position trajectory of the particle trapped in a single antinode. The inward spiral indicates damping with a much tighter spiral as the particle approaches $x = 0$, indicating a weaker frictional force as the particle approaches the antinode. It was shown previously through simulations that atoms can be cooled more rapidly in cavity cooling schemes if the laser input intensity is lowered as the particle is cooled [22]. This can now be seen to be due to the position dependence of the damping rate. For high intensities the particle is tightly confined and the amplitude of the oscillations are small resulting in a lower cooling rate. To illustrate the differences in cooling time for a constant intensity field, we plot the amplitude of the oscillating kinetic energy of the particle as a function of time for a constant intensity of 1 mW input into the cavity and for an exponentially decaying input field, initially at 1 mW, with a time constant of 50 ms. We note that the lowest intensity that can be used is limited by gravity since eventually the well depth of the intracavity field becomes less than the gravitational potential. This occurs in Fig. 5 at approximately 0.35 s. Here, the cavity intensity must be held constant and the cooling rate will be slower.

III. COOLING IN 2D

We now consider the experimentally more realistic situation of cooling in a cavity that has field variations in the axial and in the radial directions. We now must also consider motion in the radial direction as well. For this case we assume the field input into the cavity is that of the lowest-order transverse electromagnetic mode

$$E(r,x,t) = A(t)\frac{\omega_0}{\omega(x)}e^{-\frac{r^2}{\omega(x)^2}}e^{-i[\frac{kr^2}{2R(x)}+kx-\eta]}, \tag{9}$$

where $\omega_0 = \sqrt{L/k}$, $R(x) = \frac{1}{x}(x^2 + x_0^2)$, $\eta = \arctan\frac{x}{x_0}$, and $\omega(x) = \omega_0\sqrt{1+(\frac{x}{x_0})^2}$. We require that the nanosphere is trapped at the center of the cavity where the intracavity intensity is highest. At this position $(x_0 = L/2)$ $\omega(x) \approx \sqrt{2}\omega_0$, $R(x) \approx 2x_0$ and $\eta \approx \frac{\pi}{4}$. It is useful to recast this in trigonometric form as $E(r,x,t) = \frac{\xi}{2}\exp(-\frac{r^2}{\Lambda^2})[\cos kx(\cos\frac{r^2}{\Lambda^2} + \sin\frac{r^2}{\Lambda^2}) - \sin kx(\sin\frac{r^2}{\Lambda^2} - \cos\frac{r^2}{\Lambda^2})]e^{-i\omega_p t} + \text{c.c.}$, where $\Lambda = (2L/k)^{1/2}$.

The temporal evolution of the field amplitude within a cavity for a particle at coordinates (x_n, r_n) is then determined from the 2D wave equation under the slowly varying envelope approximation as for the previous 1D case. This is now given by

$$\frac{\partial\xi}{\partial t} = -\{\kappa - i[U(x_n,r_n) + \Delta]\}\xi + \kappa_{\text{ext}}\frac{\Lambda_{\text{ext}}^2}{\Lambda^2}\xi_{\text{ext}}. \tag{10}$$

All other variables are the same as for the 1D case except that $U(x_n,r_n) = \frac{\alpha\omega_p F(x_n,r_n)}{\pi\epsilon_0\Lambda^2 L}$ and $F(x_n,r_n) = e^{-\frac{r_n^2}{\Lambda^2}}[\cos^2 kx_n(\cos\frac{r_n^2}{\Lambda^2} + \sin\frac{r_n^2}{\Lambda^2}) - \frac{1}{2}\sin 2kx_n(\cos\frac{r_n^2}{\Lambda^2} - \sin\frac{r_n^2}{\Lambda^2})]$.

The rate of change of the momentum and position in the axial and radial directions within the cavity, again omitting for convenience the subscript n, is given as

$$\frac{dP_x}{dt} = -\alpha k|\xi|^2 e^{-\frac{2r^2}{\Lambda^2}}\left[\sin(2kx)\sin\frac{2r^2}{\Lambda^2} - \cos(2kx)\cos\frac{2r^2}{\Lambda^2}\right] - mg, \tag{11}$$

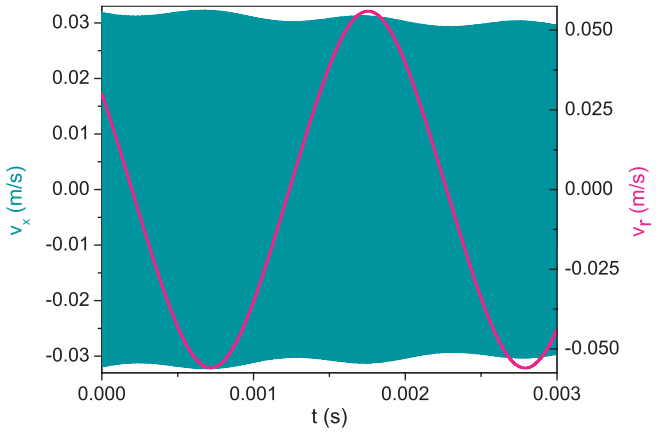

FIG. 6. (Color online) Plots illustrating the evolution in the axial and radial velocity of the trapped sphere. The axial velocity has a period of 8.2 microseconds and the radial velocity a period of 2.2 ms. The reduction in the amplitude of the axial oscillation indicates cooling over this small time period.

$$\frac{dP_r}{dt} = -2\alpha|\xi|^2\frac{r^2}{\Lambda^2}e^{-\frac{2r^2}{\Lambda^2}}\left[1+\cos(2kx)\left(\sin\frac{2r^2}{\Lambda^2} - \cos\frac{2r^2}{\Lambda^2}\right) + \sin(2kx)\left(\sin\frac{2r^2}{\Lambda} + \cos\frac{2r^2}{\Lambda^2}\right)\right], \tag{12}$$

$$\frac{dx}{dt} = P_x/m, \tag{13}$$

$$\frac{dr}{dt} = P_r/m. \tag{14}$$

These equations describe the axial and radial oscillations of the nanosphere coupled by the intracavity field, which also acts to damp the motion in both directions. We integrate these equations in time using the Runga-Kutta scheme for a nanosphere ($r = 100$ nm) trapped in a cavity operating in the fundamental TEM_{00} mode. An optical field of wavelength 1064 nm and power of 1 mW is input into the cavity with a cavity spot size of $\Lambda = 58\ \mu$m. The cavity has $\kappa = 4.7 \times 10^6$ rad/s and a length of 1 cm. Figure 6 is a plot of the axial and radial velocities of the nanosphere as a function of time with initial conditions of $x = 100$ nm, $r = 15\ \mu$m, and $v_x = v_r = 3$ cm/s. Oscillation frequencies of 476 Hz (radial) and 122 kHz (axial) result from this fixed intracavity intensity (3.8×10^9 Wm^{-2}) and cavity geometry. The very different frequencies result from the large difference in the axial and radial field gradients at the center of the cavity. Note that in this figure the fast axial motion is modulated by the slower radial motion via the cavity field. This small modulation of the cavity field by this motion is shown in Fig. 7. The cavity detuning for these simulations was chosen to be $\Delta_c = -\alpha\omega_p/\epsilon_0 V - \kappa$, optimized for cooling of the axial motion. The radial motion can be more effectively cooled by a smaller detuning.

Figure 8 is a plot of the absolute value of the envelope of the oscillatory velocity of each degree of freedom as a function time. Note that the radial cooling is much slower than in the axial direction. This is as expected from the simple 1D analysis, which shows that the damping rate is proportional to the square of the oscillation frequency. Here the radial frequency is more than two orders of magnitude less than

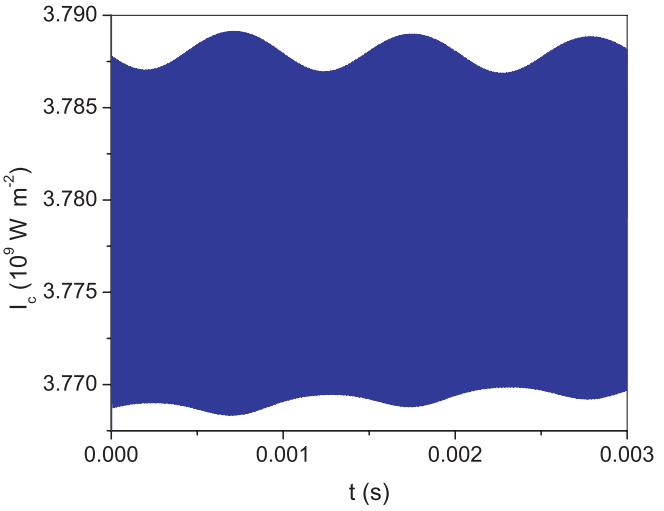

FIG. 7. (Color online) A plot of intracavity intensity calculated for the first 3 ms of cooling. The fast modulation of intensity with a period of 4.1 microseconds (not resolved) is due to the axial motion of the particle in the cavity field. The slower modulation with a period of 1.1 ms is due to the radial motion of the particle. The axial and radial motion as shown in Fig. 6. oscillates at the half the frequency of the intensity modulation.

the axial frequency. To verify this we artificially increased the radial gradient while keeping the intensity constant so that the radial frequency is the same as the axial frequency. In this case both degrees of freedom cool at approximately the same rate. It is well known that coupled oscillators or pendulums typically establish a constant phase difference depending on whether the coupling is damped or undamped. We simulated the cooling of the nanosphere for both a fixed input intensity and with a decaying intensity with a time constant of 50 ms. The cooling of both degrees of freedom is shown in a plot of the total kinetic energy as a function of time in Fig. 9. This figure clearly demonstrates that the nanosphere can be cooled with a decaying input intensity and constant input intensity. As before, the cooling rate is faster with a decaying intracavity

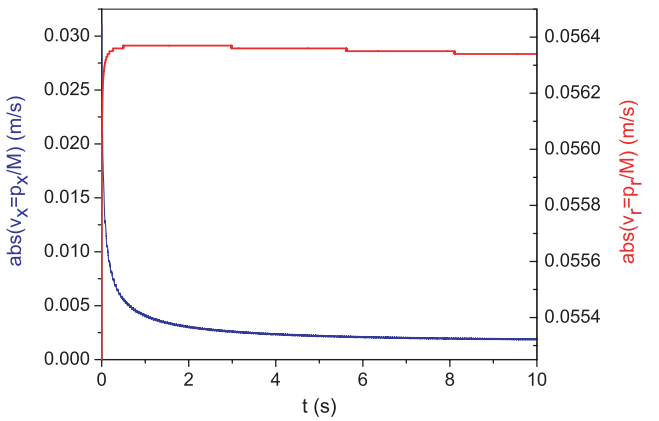

FIG. 8. (Color online) A plot of the amplitude of the oscillatory velocity of the particle for both the axial (v_x) and radial (v_r) oscillatory motion as a function of time for an input field of constant intensity. The lower curve which more rapidly decays is the axial velocity while the upper curve is the radial velocity.

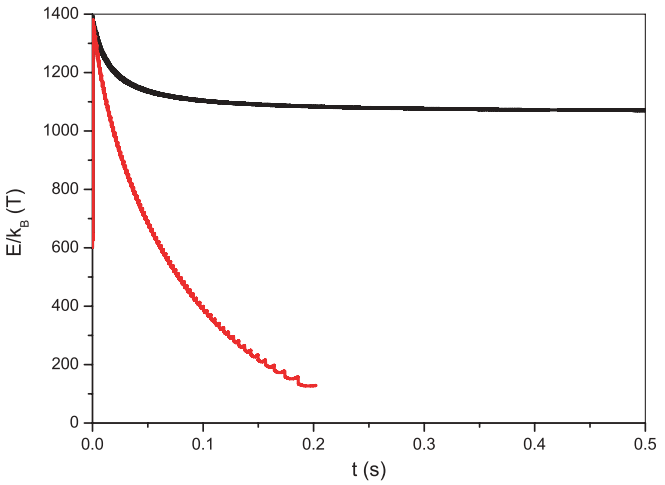

FIG. 9. (Color online) Plots of the decay of the amplitude of oscillating total kinetic energy in the cavity as a function of time, including both axial and radial motions. The upper curve, which slowly decays, is for a fixed input intensity while the lower curve is for an exponential decaying input intensity with a time constant of 50 ms.

intensity until the particle can no longer be trapped by the field, at $t = 0.2$ s in this case. An external potential, which supports the particle against gravity, will allow more rapid cooling to lower temperatures. This can be another optical field that is not resonant with the cavity field or a nanoscale charged particle within an ion trap [24,25]. The cooling of the particle can be monitored by observing scattered light or the light transmitted through the cavity. A Fourier transform of the light will show the motional sidebands for both degrees of freedom, the amplitude of which will decrease as the particle cools.

IV. CONCLUSION

We show that cooling nanoscale dielectric particles is feasible in the classical regime using cavity cooling. Such a scheme is attractive because it only relies on the optical path length change induced by a polarizable particle in the cavity and since all particles are polarizable, the scheme is potentially amenable to more complex massive particles and requires no detailed knowledge of the internal structure. The interaction between the light and the particle must be strong enough to appreciably detune the cavity. For single atoms and ions the enhanced interactions were achieved by operating near an internal electronic resonance. Although larger nanoscale particles usually do not have discrete internal energy levels, they do have large static polarisabilities, which scale with particle volume. It is precisely this feature that allows a single nanoscale particle to be cooled in high-finesse cavities ($F \approx 10^4$) using fields that are not near a resonance. We show cooling times on the order of seconds to minutes appear feasible for both axial and radial center-of-mass motions. While we do not include the effects of absorption of light, which will heat the particle, early experiments by Ashkin suggested that microscale dielectric particles can be held for durations of 30 min before they are expelled from the field by radiometric forces [24]. These forces will be much less important in nanoscale dielectric particles since the particle will have a more uniform temperature. The effects of gas collisions must also be included in future work, as well as the finite size of the particle. The latter will slow the cooling process because the effective gradient in the axial potential will be smaller. Finally, these particles can also be cooled in the resolved-sideband limit, which for a fixed cavity geometry and reflectivity can be controlled by laser input intensity. In this regime cooling to the quantum limit is feasible and will be the goal of future work.

[1] J. D. Teufel, J. W. Harlow, C. A. Regal, and K. W. Lehnert, Phys. Rev. Lett. **101**, 197203 (2008).
[2] R. G. Knobel and A. N. Cleland, Nature (London) **424**, 291 (2003).
[3] S. Etaki *et al.*, Nature Phys. **4**, 785 (2008).
[4] C. H. Metzger and K. Karrai, Nature (London) **432**, 1002 (2004).
[5] V. B. Braginskii, Sov. Phys. JETP **26**, 831 (1968).
[6] M. D. LaHaye, O. Buu, B. Camarota, and K. C. Schwab, Science **304**, 74 (2004).
[7] W. Marshall, Ch. Simon, R. Penrose, and D. Bouwmeester, Phys. Rev. Lett. **91**, 130401 (2003).
[8] K. Jensen, K. Kim, and A. Zetti, Nature Nanotechnology **3**, 533 (2008).
[9] T. J. Kippenberg and K. J. Vahala, Science **321**, 1172 (2008).
[10] A. Schliesser, O. Arcizet, R. Riviére, G. Anetsberger, and T. J. Kippenberg, Nature Physics **5**, 509 (2009).
[11] J. D. Thompson *et al.*, Nature (London) **452**, 72 (2008).
[12] D. K. Armani, T. J. Kippenberg, S. M. Spillane, and K. J. Vahala, Nature (London) **421**, 925 (2003).
[13] P. Horak, G. Hechenblaikner, K. M. Gheri, H. Stecher, and H. Ritsch, Phys. Rev. Lett. **79**, 4974 (1997).
[14] V. Vuletic and S. Chu, Phys. Rev. Lett. **84**, 3787 (2000).
[15] F. A. Narducci, Z. Ye, and H. Y. Ling, J. Mod. Opt. **49**, 687 (2002).
[16] P. Maunz, T. Puppe, I. Schuster, N. Syassen, P. W. H. Pinkse, and G. Rempe, Nature (London) **428**, 50 (2004).
[17] D. R. Leibrandt, J. Labaziewicz, V. Vuletic, and I. L. Chuang, Phys. Rev. Lett. **103**, 103001 (2009).
[18] H. W. Chan, A. T. Black, and V. Vuletic, Phys. Rev. Lett. **90**, 063003 (2003).
[19] J. D. Thompson, B. M. Zwickl, A. M. Jayich, F. Marquardt, S. M. Girvin, and J. G. E. Harris, Nature (London) **452**, 72 (2008).
[20] G. Hechenblaikner, M. Gangl, P. Horak, and H. Ritsch, Phys. Rev. A **58**, 3030 (1998).
[21] A. Liénard, Revue Generale de l'Electricite **23**, 901 (1928).
[22] W. Lu and P. F. Barker, Phys. Rev. A **72**, 025402 (2005).
[23] I. Wilson-Rae, N. Nooshi, W. Zwerger, and T. J. Kippenberg, Phys. Rev. Lett. **99**, 093901 (2007).
[24] A. Ashkin and J. M. Dziedzic, Appl. Phys. Lett. **28**, 333 (1976).
[25] S. Schlemmer, J. Illemann, S. Wellert, and D. Gerlich, J. Appl. Phys. **90**, 5410 (2001).